Integrated Single-cell Bioinformatics Analysis Reveals Intrinsic and Extrinsic Biological Characteristics of Hematopoietic Stem Cell Aging

Xiangjun Zeng
  First Hospital of Zhejiang Province: Zhejiang University School of Medicine First Affiliated Hospital
Xia Li
  First Hospital of Zhejiang Province: Zhejiang University School of Medicine First Affiliated Hospital
Mi Shao
  First Hospital of Zhejiang Province: Zhejiang University School of Medicine First Affiliated Hospital
Yulin Xu
  First Hospital of Zhejiang Province: Zhejiang University School of Medicine First Affiliated Hospital
Wei Shan
  First Hospital of Zhejiang Province: Zhejiang University School of Medicine First Affiliated Hospital
Cong Wei
  First Hospital of Zhejiang Province: Zhejiang University School of Medicine First Affiliated Hospital
Xiaoqing Li
  First Hospital of Zhejiang Province: Zhejiang University School of Medicine First Affiliated Hospital
Limengmeng Wang
  First Hospital of Zhejiang Province: Zhejiang University School of Medicine First Affiliated Hospital
Yongxian Hu
  First Hospital of Zhejiang Province: Zhejiang University School of Medicine First Affiliated Hospital
Yanmin Zhao
  First Hospital of Zhejiang Province: Zhejiang University School of Medicine First Affiliated Hospital
Pengxu Qian
  Zhejiang University School of Medicine
He Huang (✉ huanghe@zju.edu.cn)
  First Hospital of Zhejiang Province: Zhejiang University School of Medicine First Affiliated Hospital   https://orcid.org/0000-0002-2723-1621

Abstract

Hematopoietic stem cell (HSC) aging, which is accompanied by loss of self-renewal capacity, myeloid-biased differentiation and increased risks of hematopoietic malignancies, is an important focus in stem cell research. However, the mechanisms underlying HSC aging have not been fully elucidated. In the present study, we integrated 3 independent single-cell transcriptome datasets of HSCs together and identified Il10ra and Tnfsf14 as two markers of inflammatory and apoptosis-biased aged HSCs. Besides, common differentially expressed genes (DEGs) between young and aged HSCs were identified and further validated by quantitative RT-PCR. Functional enrichment analysis revealed that these DEGs were predominantly involved in the cell cycle and the tumor necrosis factor (TNF) signaling pathway. We further found that the Skp2-induced signaling pathway (Skp2→Cip1→CycA/CDK2→DP-1) contributed to a rapid transition through G1 phase in aged HSCs. In addition, analysis of the extrinsic alterations on HSC aging revealed the increased expression levels of inflammation genes in bone marrow microenvironment. Colony formation unit assays showed that inflammatory cytokines promoted cellular senescence and that blockade of inflammatory pathway markedly rejuvenated aged HSC functions and increased B cell output. Collectively, our study elucidated the biological characteristics of HSC aging, and the genes and pathways we identified could be potential biomarkers and targets for the identification and rejuvenation of aged HSCs.

Background

Hematopoietic stem cell (HSC) aging is accompanied by reduced self-renewal ability, myeloid-biased differentiation, impaired homing capacity and other defects in hematopoietic reconstitution function [1−4]. Emerging studies have elucidated the intrinsic and extrinsic mechanisms of HSC aging. For instance, microarray analysis of HSC expression profiles revealed that HSC aging was accompanied by downregulation of genes mediating lymphoid specification differentiation and upregulation of genes involved in specifying myeloid fate [1]. Studies of the cell-extrinsic bone marrow niche indicated that dysfunction of aged marrow macrophages directed HSC platelet bias and that aged mice exhibited markedly more senescent neutrophils than young mice [5].

Most of the traditional knowledge about HSC aging relies on bulk RNA sequencing, which generates an averaged landscape but underestimates the true heterogeneity of cells [6]. In addition, the required number of cells for bulk RNA sequencing is large, and it is difficult to generate transcriptome profiles for rare cells including HSCs. With the rapid development of single-cell RNA sequencing technology, the dissection of gene expression has provided unprecedented insights into cellular heterogeneity [7]. On the one hand, several studies have characterized distinct transcriptome profiles of young and aged HSCs at single-cell resolution and revealed cell-intrinsic differences during HSC aging [5, 8, 9]. On the other hand, cell-extrinsic mechanisms were also revealed by the single cell transcriptome profiles of young and aged bone marrow niches in different studies [10, 11]. However, these results were all based on a single study respectively and lacked reproducibility, consistency and comparability. To overcome these shortcomings, integrated bioinformatics methods should be utilized to further elucidate the mechanisms underlying HSC aging.

In the present study, 3 independent single-cell transcriptome datasets [5, 8, 9] of purified young and aged HSCs were integrated together and cellular heterogeneity analysis was performed to illustrate the differences of subpopulations within HSCs. Besides, common differentially expressed genes (DEGs) between young and aged HSCs were identified and further validated by real-time quantitative reverse transcription PCR (qRT-PCR). Then, several bioinformatics methods, including functional enrichment analysis and protein−protein interaction (PPI) network analysis, were used to profoundly explore the effects and functions of these DEGs. Furthermore, 2 single-cell transcriptome datasets of the bone marrow niche [10, 11] were also employed to analyze cellular composition and the interactions between HSCs and other cell types in the bone marrow. Finally, to confirm the increased level of inflammation, a Cytoplex Assay was performed to measure the levels of inflammation-related cytokines and chemokines in young and aged bone marrow and colony formation unit (CFU) assays were performed to assess the effect of inflammatory cytokines on cellular senescence. Our study elucidated the biological characteristics of HSC aging, and the genes and pathways we identified could be potential biomarkers and targets for the identification and rejuvenation of aged HSCs.

Materials And Methods

Dataset integration, data scaling, dimension reduction and clustering

Three datasets of HSC expression profiles from young and aged mice (GSE100906, GSE70657 and GSE100426, dataset information is shown in Supplementary Table 1) were downloaded from the Gene Expression Omnibus database (http://www.ncbi.nlm.nih.gov/geo). To minimize batch effect between datasets, we integrated 3 datasets following the procedure of Seurat 3 [12, 13]. Briefly, the highly variable genes for each dataset were selected with the FindVariableFeatures function and the top highly variable 2000 genes were thus integrated by iteratively merging pairs of datasets according to a given distance. Integration anchors were done using the FindIntegrationAnchors function (dims = 1:30) and dataset was corrected using IntegrateData function (dims = 1:30). This process resulted in an expression matrix that contains the batch-effect-corrected expression for the 2000 selected genes of the cells from the 3 samples. Scaling expression values with cell to cell variations were obtained with the ScaleData function of Seurat. A PCA was performed on the scaled data using RunPCA function (npcs = 30) and the principal components of the PCA were kept for nonlinear dimension reduction and cell clustering by t-Distributed Stochastic Neighbor Embedding (t-SNE). The FindNeighbors and FindClusters Seurat functions were used to cluster the cells with the Louvain algorithm (resolution = 0.8).

DEGs identification and validation by Multi-cell one-step PCR assay

DEG identification was performed using the package DESeq2 [14]. |Foldchange| > 1.5 and $p < 0.05$ were set as the cutoffs to screen for DEGs. LT-HSCs (Lineage-Sca1 + c-Kit + CD150 + CD48-) were collected with an SH800S Cell Sorter from the bone marrow of young (4 ~ 6 weeks, n = 3, C57BL/6) and aged (18 ~ 20 months, n = 3, C57BL/6) mice, and the gene expression of the LT-HSCs was determined using multi-cell one-step PCR. Briefly, LT-HSCs were transferred into 8-well PCR strips loaded with One-Step PCR Master Mix in each well (Vazyme, Nanjing, China), and the strips were frozen at − 80°C for 5 min. Reverse

transcription was performed at 50°C for 60 min. Pre-denaturation was achieved by heating to 95°C for 3 min. Subsequently, the cDNA was subjected to 15 cycles of sequence-specific amplification via denaturing at 95°C for 15 s and annealing and elongation at 60°C for 15 min. Detection of gene expression from the amplified cDNA was performed using a LightCycler® 480 (Roche, Basel, Switzerland). The primer sets for the detection of DEGs are listed in Supplementary Table 3.

Functional enrichment and PPI network analysis of DEGs

Functional enrichment analysis of DEGs was performed with DAVID (https://david-d.ncifcrf.gov/), including Gene Ontology (GO) term enrichment and Kyoto Encyclopedia of Genes and Genomes (KEGG) pathway enrichment [15, 16]. GO term categories included biological process (BP), molecular function (MF) and cellular component (CC). STRING (http://string-db.org), a web database recording physical and functional protein–protein interaction information, was used to predict the interactions among DEGs [17]. Cytoscape software was applied to establish the protein interaction network [18]. MCODE, a plug-in in Cytoscape, was utilized to screen the modules from the PPI network and identify the most significant module based on the MCODE score and node number [19]. CytoHubba, a plug-in in Cytoscape, was utilized to explore important nodes/hubs in the interactome network [20].

Clustering-based analysis of cell cycle state

The cell cycle phase (G1, S, or G2M) of each cell was identified by calculating the cell cycle phase score based on canonical markers using the Seurat package (version 3.1)[12, 13]. The canonical cell cycle gene set was defined with "cell cycle process" from the GO annotation and identified as cycling in HeLa cells [21] and it can be downloaded from GSEA MSigDB version 7.1 (https://www.gsea-msigdb.org/gsea/msigdb) [22, 23].

Analysis of interactions between HSCs and surrounding cells in the bone marrow niche

The single cell transcriptome profiles of young and aged mouse bone marrow based on the microfluidic droplet platform (10x Genomics) were shared by the Tabula Muris Consortium (tabula-muris-senis.ds.czbiohub.org) [10, 11]. For cellular interaction analysis, CellphoneDB software (version 2.0) was used [24, 25] with the default parameters. Significant ligand–receptor pairs were filtered with $p < 0.05$. To identify which cell population accounted for the difference in inflammation-related cytokine levels, CellChat software was applied to analyze outgoing communication patterns of secreting cells [26].

Quantitation of inflammation-related cytokines and chemokines via a Cytoplex Assay

LEGENDPlex assays (Mouse Proinflammatory Chemokine Panel and Mouse Inflammation Panel; BioLegend) were performed to monitor cytokine and chemokine levels of bone marrow from young (4 ~ 6 weeks, n = 3, C57BL/6) and aged (18 ~ 20 months, n = 3, C57BL/6) mice. The femurs and tibias were cut at both ends, and the bone marrow was flushed out with 1 ml PBS. The suspension was centrifuged at 1,500 rpm for 5 min, and the supernatant was collected. Twenty-five microliters of supernatant was used for the protocol following the manufacturer's instructions. Samples were analyzed by flow cytometry on an Attune NxT Flow Cytometer (BD Biosciences), and the data were analyzed using LEGENDPlex software (BioLegend).

Colony formation unit assay:

Colony formation unit assays were performed as follows. 100 FACS-isolated HSCs (Lineage-Sca1 + c-Kit+) from young (4 ~ 6 weeks, n = 3, C57BL/6) and aged (18 ~ 20 months, n = 3, C57BL/6) mice were plated in methylcellulose (M3434 for BFU-E, CFU-GM, CFU-GEMM measurement and M3630 for CFU-B measurement, Stem Cell Technologies) and enumerated on day 10. To test the effect of inflammatory cytokines on hematopoietic cell lineage, either DMSO vehicle or IL-1β (25 ng/ml), TNF-α (1 μg/ml), AS101 (2μg/ml, IL-1β inhibitor) and R7050 (2μg/ml, TNF-α receptor antagonist) were added to the methylcellulose media. All cultures were performed at 37°C in a 5% CO_2 water jacket incubator.

Results

Cellular heterogeneity within young and aged HSCs

To characterize the differences in HSC subpopulations, three datasets of HSC single cell expression profiles from young and aged mice were integrated together using Seurat [12, 13] to correct batch effect (dataset information is shown in Supplementary Table 1). Reduction of dimension and unsupervised clustering were performed using t-Distributed Stochastic Neighbor Embedding (t-SNE). A total of 5 clusters were identified (Fig. 1A, B), which were characterized further by identifying their markers using DEG analysis on the log-normalized data without any correction and by deducing their characteristics from gene set enrichment analysis (Fig. 1C, E). To assess the aging effect at the level of HSC populations, we compared the proportion of different clusters in young and aged HSCs (Fig. 1D). Interestingly, Cluster 2, a self-renewal-associated cluster marked by Ccnb1, decreased significantly upon aging. Besides, Cluster 3 (an inflammation-associated cluster marked by Il10ra) and Cluster 4 (an apoptosis-associated cluster marked by Tnfsf14) were increased upon aging. Tnfsf14 is a proapoptotic member of the TNF ligand family and promotes myeloid differentiation of HSCs [27]. As a whole, these results highlighted an exhaustion of HSCs being able to give rise to HSC itself without differentiation, which is a hallmark of HSC aging and indicated that Il10ra and Tnfsf14 were two markers for accumulation of inflammatory and apoptosis-biased state HSCs.

Identification of DEGs between young and aged HSCs

In order to elucidate the overall alterations of HSC aging, we next analyzed HSCs as a whole. According to the cut-off criterion (|Foldchange| > 1.5 and $p <$ 0.05), 453, 614 and 297 DEGs between young and aged HSCs were identified from GSE100906, GSE70657 and GSE100426, respectively (Fig. 2A). Common DEGs were defined as genes that were significantly upregulated or downregulated in at least two datasets. By employing integrated bioinformatics analysis, 56 common upregulated genes and 51 common downregulated genes were identified (Fig. 2B, Supplementary Table 2). For instance, *Birc5* and *Kpna2* were downregulated, while *Clu*, *Selp* and *Sdpr* were upregulated in HSCs during aging. To confirm the results of common DEGs, the relative expression levels of top

30 DEGs were analyzed by qRT-PCR (Fig. 2C). We found that the PCR results for approximately 75% of the genes were consistent with our bioinformatics analysis ($p < 0.05$).

Functional enrichment analysis of DEGs

To further delineate the functional changes that occur during HSC aging, functional enrichment of the common DEGs was performed by using the DAVID gene annotation tool (Fig. 3A). For BP, the upregulated genes were mainly enriched in transcription, DNA-templated and regulation of transcription from RNA polymerase II promoter, and the downregulated genes were predominantly enriched in cell cycle, mitotic nuclear division, cell division and protein phosphorylation. This was consistent with the previous findings that cell cycle-related genes dominated the transcriptomic variability of aging and that aged HSCs underwent fewer cell divisions than young HSCs [28–30]. KEGG pathway enrichment analyses revealed that the upregulated DEGs were mainly involved in osteoclast differentiation and TNF signaling pathway, and the downregulated DEGs were mainly involved in cell cycle, oocyte meiosis and p53 signaling pathway. p53 is implicated in regulating HSC aging and quiescence [31] and regulating p53 can help to maintain hematopoietic cells by regulating intracellular ROS during oxidative stress [32]. These results highlighted the loss of self-renewal ability and quiescence in aged HSCs.

PPI network analysis of DEGs

To better understand the interactions among the common DEGs, a PPI network with 67 nodes (27 upregulated and 40 downregulated) and 413 edges was generated with the STRING tool (Fig. 3B). Two significant modules were also identified based on the degree of importance in Cytotype MCODE. Module 1 contained 25 nodes and 286 edges (Fig. 3C), and the expression of all the nodes was downregulated in aged HSCs. KEGG pathway enrichment analyses revealed that the DEGs in Module 1 were mainly enriched in the cell cycle. Module 2 contained 11 nodes and 17 edges (Fig. 3D), and the DEGs in Module 2 were mainly enriched in cell adhesion molecules and the hematopoietic cell lineage. In addition, highly connected nodes with a large number of edges in the network are likely to have significant functional importance and were defined as hub genes. By utilizing CytoHubba in Cytotype, we identified the top 5 upregulated hub genes (*Jun, Aldh1a1, Egr1, Cd38* and *Junb*) and the top 5 downregulated hub genes (*Aurka, Ccna2, Ccnb2, Cdk1* and *Birc5*). The alterations and potential functions of the hub genes were summarized in Table 1.

Table 1
Alterations and functions of hub genes during aging

Gene	Aliase	Alterations with Age	Functions
Aurka	Aurora kinase A	Down	Contributed to the regulation of cell cycle progression.
Ccna2	Cyclin-A2	Down	Controlled both the G1/S and the G2/M transition phases of the cell cycle.
Ccnb2	G2/mitotic-specific cyclin-B2	Down	Essential for the control of the cell cycle at the G2/M transition.
Cdk1	Cyclin-dependent kinase 1	Down	Essential for the control of the eukaryotic cell cycle, promoted G2-M transition, and regulated G1 progress and G1-S transition.
Birc5	Baculoviral IAP repeat-containing protein 5	Down	Had dual roles in promoting cell proliferation and preventing apoptosis.
Jun	Transcription factor AP-1	Up	Regulated functional development of hematopoietic precursor cells into mature blood cells.
Aldh1a1	Retinal dehydrogenase 1	Up	Regulated retinoic acid biosynthesis, the clearance of toxic byproducts of reactive oxygen species and HSC differentiation.
Egr1	Early growth response protein 1	Up	Played a role in the regulation of cell survival, proliferation and cell death and in regulating the response to growth factors and DNA damage.
Cd38	Cluster of Differentiation 38	Up	Cell adhesion and signal transduction.
Junb	Transcription factor jun-B	Up	Involved in regulating gene activity following the primary growth factor response.

Cell cycle analysis of HSCs

As the enrichment analysis of common DEGs and PPI network analysis suggested that the cell cycle was strongly associated with functional decline in aged HSCs, we next compared the expression levels of cell cycle-associated genes. Among 107 DEGs, 24 genes were associated with the cell cycle and most of them (22 genes), including *Chek2, Kif20b* and *Clasp2*, were downregulated in at least 2 datasets (Fig. 4A). Subsequently, the cell cycle phase of young and aged HSCs was identified by calculating the cell cycle phase score based on canonical markers in both young and aged mice (Fig. 4B). The frequency of cells in the G1 cluster significantly decreased in aged versus young cells (13.5% vs 6.8%; $p < 0.05$, shown in Fig. 4C).

To further identify the signaling pathways that drove HSCs to transit through G1 phase quickly, we evaluated genetic alterations in a cell cycle pathway diagram that was publicly available at https://www.genome.jp/kegg [33]. We found that the Skp2-induced signaling pathway (Skp2→Cip1→CycA/CDK2→DP-1) was significantly downregulated during the aging process; this change promoted the synthesis of mRNAs and proteins that are required for DNA synthesis during S phase (Fig. 4D).

Analysis of the alterations in bone marrow during the aging process

The PPI network analysis confirmed significant changes of adhesion molecules, highlighting an important role of bone marrow microenvironment in the aging process. Therefore, we reanalyzed two single cell transcriptome profiles of young and aged mouse bone marrow and investigated how the cellular

composition of the bone marrow changed with age. The percentages of erythroblasts, granulocytopoietic cells and granulocytes increased with age, while the percentages of macrophages, late pro-B cells, monocytes and T cells decreased with age (Fig. 5A). Cell-cell communication mediated by receptor-ligand complexes is crucial for coordinating diverse biological processes, such as development, differentiation and responses to infection [24]. To assess changes in intercellular communication between HSCs and other cell types during aging, cellphoneDB software was used to predict interactions between the various cell types from the single-cell RNA-seq data [24, 25]. Significant predicted interactions were assessed separately for young and aged mice (Fig. 5B), and the differences were used to infer changes in intercellular interactions (Fig. 5C). The predicted interactions with hematopoietic stem/progenitor cells (HSPCs) were highest in monocytes and lowest in erythroblasts in both young and aged mice. The comparison between the young and aged groups indicated a significant increase in intercellular communication between HSPCs and proerythroblasts, and a decrease in intercellular communication between HSPCs and monocytes, granulocytopoietic cells and granulocytes (Fig. 5C).

As the surrounding cells of HSPCs are potential niche components, the ligands expressed by these populations and the receptors expressed by HSPCs were considered in the downstream analysis. Among a total of 68 heterologous ligand−receptor pairs detected between HSPCs and other cell types, immune response, inflammation response and signal transduction were the predominant biological processes involved (Fig. 5D). In addition, ligand−receptor pairs were involved in some canonical signaling pathways (such as the TNF signaling pathway, NF-kappa B signaling pathway and PI3K-Akt signaling pathway) and certain aging-associated diseases (such as Alzheimer's disease).

The ligand−receptor gene pairs exhibited differential expression patterns between young and aged populations when coupled with HSPCs. Interactions with HSPCs changed significantly in proerythroblasts, monocytes, granulocytopoietic cells and granulocytes, and the significant differentially expressed ligand−receptor gene pairs of these four groups of cells are shown in Fig. 5E. Adhesion complexes, such as aMb2 complex-Icam1 and aLb2 complex-Icam1, were differentially expressed during HSC aging. Moreover, inflammation-related ligand-receptor pairs, such as CXCL2-CXCR2, IL15-IL15 receptor, CCL2-CCR2 and CCL5-CCR5, were upregulated during HSC aging.

Analysis of inflammation levels in the bone marrow niche

The upregulated inflammation-related ligand-receptor pairs in aged HSCs suggested increasing inflammation levels in the bone marrow niche during aging. To test our hypothesis, a Cytoplex Assay was performed to measure the levels of inflammation-related cytokines and chemokines in the bone marrow. Most inflammation-related cytokines and chemokines, including TNF-α, IFN-β, IFN-γ, IL-1α, IL-1β, IL-6, IL-17α, IL-23, CCL2, CCL4 and CXCL1, were upregulated in aged bone marrow niche, while CCL20 and CXCL10 were downregulated in the aged bone marrow niche (Fig. 6A). To assess the effect of inflammatory cytokines on cellular senescence, HSCs were cultured in methylcellulose with either inflammatory cytokines or their inhibitors. TNF-α and IL-1β promoted myeloid-biased differentiation and inflammatory pathway blockade may rejuvenate aged HSC functions and increase B cell output (Fig. 6B).

To further determine which cell population accounted for the difference in inflammation-related cytokine levels, the outgoing communication patterns of secreting cells were analyzed (Fig. 6C). The secretion of HSPCs, erythroblasts and basophils contributed to high CCL levels in the aged bone marrow niche, while the secretion of T cells, promonocytes, macrophages, erythroblasts, and basophils contributed to high IFN-γ levels. In addition, the secretion of some interleukins and complement factors was upregulated in proerythroblasts and immature B cells. Interestingly, the levels of inflammation-related cytokines secreted by HSPCs, including CCL and IL2, were increased, highlighting the important role of autocrine signaling during aging process. Circle plots of the cell-cell communication network also revealed that inflammatory pathway networks (such as IL2, CCL and complement; Fig. 6D, Supplementary Fig. 1A) became more interconnected during aging, with some ligand-receptor communication enhanced significantly (such as IL2 - IL2RB/IL2RG and CCL5 - CCR1; Supplementary Fig. 1B).

Discussion

HSC aging is a comprehensive result of both intrinsic and extrinsic factors. To illustrate the biological characteristics of HSC aging, we integrated 3 independent single-cell transcriptome datasets of HSCs together and identified cellular heterogeneity within HSCs. Common DEGs between young and aged HSCs were identified and confirmed by qRT-PCR, and several bioinformatics methods were employed to profoundly explore the biological functions of DEGs. Besides, we compared the cellular composition of the bone marrow, analyzed intercellular communication between HSCs and other cell types and identified important differentially expressed ligand-receptor pairs. Furthermore, we measured the levels of some inflammation-related cytokines in the bone marrow niche and determined which cell population accounted for high inflammation-related cytokine levels in aged bone marrow.

First, we identified two HSCs subsets (Il10ra + inflammation-associated HSCs and Tnfsf14 + apoptosis-associated HSCs) that accumulated significantly with aging. Consistently, it was reported that both Il10 and Tnfsf14 regulated myeloid differentiation of HSCs [27, 34], indicating Il10ra and Tnfsf14 to be markers of dysfunctional aged HSCs. Besides, functional enrichment of DEGs revealed that the downregulated genes were predominantly involved in the cell cycle (Fig. 3). Consistent with our findings, previous studies have shown that the cell cycle activity of HSCs declines during the aging process, with aged HSCs undergoing fewer cell divisions than young HSCs [28, 29]. Further analysis revealed that the number of cells in G1 phase decreased in aged HSCs (Fig. 4) and that downregulation of the Skp2-induced signaling pathway (Skp2→Cip1→CycA/CDK2→DP-1) in aged HSCs promoted the transition from G1 phase to S phase. Skp2 is the F-box protein component of an SCF-type ubiquitin ligase that interacts specifically with p27Kip1 and thereby promotes its ubiquitylation and degradation, which plays an important role in cell cycle progression from G1 to S phase [35, 36]. Recently, a study on endothelial progenitor cells reported that depletion of Skp2 generated a senescent bioenergetic profile, whereas adenoviral-mediated Skp2 expression reversed this senescence [37]. Therefore, the Skp2-induced signaling pathway may promote alterations in the distribution of cells in different cell cycle stages and activation of this signaling pathway may promote rejuvenation of aged HSCs.

In addition, the upregulated genes were predominantly involved in the TNF signaling pathway (Fig. 3D). Consistent with this, some inflammation-related ligand-receptor pairs (such as CXCL2-CXCR2, CCL2-CCR2 and CCL5-CCR5) and most of the inflammation-related cytokines and chemokines in the bone

marrow niche were upregulated during aging (Fig. 6A). Previous reports have demonstrated that a state of chronic inflammation is correlated with aging and is a strong risk factor for the occurrence of many chronic diseases [38−41]. However, the exact mechanisms underlying the increase in inflammatory factors are not completely understood. By utilizing single cell transcriptome data, expression of inflammatory cytokines in different cell populations can be revealed. For instance, the secretion of HSPCs, erythroblasts and basophils contributed to high CCL levels in the aged bone marrow niche, while the secretion of T cells, promonocytes, macrophages, erythroblasts, and basophils contributed to high IFN-γ levels. In addition, the levels of inflammation-related signaling molecules secreted by HSPCs were increased, highlighting the important role of autocrine signaling during the aging process. Consistently, it was reported that direct Toll-like receptor activation in HSPCs resulted in the production of proinflammatory cytokines such as IL-6, in either a paracrine or an autocrine manner, and enhanced proliferation and myeloid differentiation under neutropenic conditions in vivo [42]. Taken together, these findings indicated that both autocrine signals from HSPCs themselves and paracrine signals played important roles in the high levels of inflammation in the aged bone marrow niche.

Conclusion

Utilizing an integrated single-cell bioinformatics analysis, we elucidated intrinsic and extrinsic biological characteristics of HSC aging. Analysis of cellular heterogeneity identified Il10ra and Tnfsf14 as two markers of inflammatory and apoptosis-biased aged HSCs. The common DEGs between young and aged HSCs were predominantly enriched in the cell cycle, the TNF signaling pathway, the hematopoietic cell lineage and cell adhesion molecules. Cell cycle activity decreased during the aging process and the Skp2-induced signaling pathway (Skp2→Cip1→CycA/CDK2→DP-1) contributed to a rapid transition through G1 phase in aged HSCs. In addition, evaluation of the bone marrow microenvironment demonstrated that most inflammation-related cytokines (such as TNF-α, IFN-β, IFN-γ and IL-1α) were upregulated during the aging process and identified the sources of these inflammation-related cytokines. Colony formation unit assays showed that inflammatory cytokines promoted cellular senescence and that blockade of inflammatory pathway markedly rejuvenated aged HSC functions and increased B cell output. Our study elucidated the molecular mechanisms underlying HSC aging, and the genes and pathways we identified could be potential biomarkers and targets for the identification and rejuvenation of aged HSCs.

Abbreviations

Hematopoietic stem cell (HSC); Differentially expressed gene (DEG); Tumor necrosis factor (TNF); real-time quantitative reverse transcription PCR (qRT-PCR); Protein−protein interaction (PPI); Colony formation unit (CFU); Hematopoietic stem/progenitor cell (HSPC); Gene Expression Omnibus (GEO); Gene Ontology (GO); Kyoto Encyclopedia of Genes and Genomes (KEGG); Biological process (BP); Molecular function (MF); Cellular component (CC);

Declarations

Author contributions

XZ, XL and MS analyzed the data, performed experiments, and wrote the manuscript. YX, WS, CW and XL helped to performed the Cytoplex Assay. LW, YH, YZ, PQ and HH provided suggestions and revisions. All authors contributed to the writing of the article. All authors read and approved the final manuscript.

Ethics approval and consent to participate

All animal experiments were carried out in accordance with approved animal protocols, the guideline and ethical approval of the Institutional Animal Care and Use Committee of ZJU.

Consent for publication

Not applicable.

Acknowledgement

Not applicable.

Availability of data and material

The single cell RNA sequencing data of HSCs that supports the findings of this study is available in GEO at https://www.ncbi.nlm.nih.gov/geo/ (GSE100906, GSE70657 and GSE100426). The data of bone marrow niche that supports the findings of this study is available on Figshare (https://figshare.com/projects/Tabula_Muris_Transcriptomic_characterization_of_20_organs_and_tissues_from_Mus_musculus_at_single_cell_resolution/273 and GitHub (https://github.com/czbiohub/tabula-murissenis). Code used for the analysis are available from GitHub (https://github.com/lixia2017/HSC-aging-pipeline).

Declaration of interests

The authors declare that there is no conflict of interests.

Funding

References

1. Rossi DJ, Bryder D, Zahn JM, Ahlenius H, Sonu R, Wagers AJ, Weissman IL: **Cell intrinsic alterations underlie hematopoietic stem cell aging.** *Proc Natl Acad Sci U S A* 2005, **102:**9194-9199.

2. Li X, Zeng X, Xu Y, Wang B, Zhao Y, Lai X, Qian P, Huang H: **Mechanisms and rejuvenation strategies for aged hematopoietic stem cells.** *Journal of Hematology & Oncology* 2020, **13:**31.

3. Dykstra B, Olthof S, Schreuder J, Ritsema M, de Haan G: **Clonal analysis reveals multiple functional defects of aged murine hematopoietic stem cells.** *J Exp Med* 2011, **208:**2691-2703.

4. Liang Y, Van Zant G, Szilvassy SJ: **Effects of aging on the homing and engraftment of murine hematopoietic stem and progenitor cells.** *Blood* 2005, **106:**1479-1487.

5. Frisch BJ, Hoffman CM, Latchney SE, LaMere MW, Myers J, Ashton J, Li AJ, Saunders J, 2nd, Palis J, Perkins AS, et al: **Aged marrow macrophages expand platelet-biased hematopoietic stem cells via Interleukin1B.** *JCI insight* 2019, **5:**e124213.

6. Goldman SL, MacKay M, Afshinnekoo E, Melnick AM, Wu S, Mason CE: **The Impact of Heterogeneity on Single-Cell Sequencing.** *Front Genet* 2019, **10:**8.

7. Ye F, Huang W, Guo G: **Studying hematopoiesis using single-cell technologies.** *Journal of Hematology & Oncology* 2017, **10:**27.

8. Grover A, Sanjuan-Pla A, Thongjuea S, Carrelha J, Giustacchini A, Gambardella A, Macaulay I, Mancini E, Luis TC, Mead A, et al: **Single-cell RNA sequencing reveals molecular and functional platelet bias of aged haematopoietic stem cells.** *Nat Commun* 2016, **7:**11075.

9. Mann M, Mehta A, de Boer CG, Kowalczyk MS, Lee K, Haldeman P, Rogel N, Knecht AR, Farouq D, Regev A, Baltimore D: **Heterogeneous Responses of Hematopoietic Stem Cells to Inflammatory Stimuli Are Altered with Age.** *Cell Rep* 2018, **25:**2992-3005.e2995.

10. Schaum N, Karkanias J, Neff NF, May AP, Quake SR, Wyss-Coray T, Darmanis S, Batson J, Botvinnik O, Chen MB, et al: **Single-cell transcriptomics of 20 mouse organs creates a Tabula Muris.** *Nature* 2018, **562:**367-372.

11. Almanzar N, Antony J, Baghel AS, Bakerman I, Bansal I, Barres BA, Beachy PA, Berdnik D, Bilen B, Brownfield D, et al: **A single-cell transcriptomic atlas characterizes ageing tissues in the mouse.** *Nature* 2020, **583:**590-595.

12. Butler A, Hoffman P, Smibert P, Papalexi E, Satija R: **Integrating single-cell transcriptomic data across different conditions, technologies, and species.** *Nature Biotechnology* 2018, **36:**411-420.

13. Stuart T, Butler A, Hoffman P, Hafemeister C, Papalexi E, Mauck WM, 3rd, Hao Y, Stoeckius M, Smibert P, Satija R: **Comprehensive Integration of Single-Cell Data.** *Cell* 2019, **177:**1888-1902.e1821.

14. Love MI, Huber W, Anders S: **Moderated estimation of fold change and dispersion for RNA-seq data with DESeq2.** *Genome Biology* 2014, **15:**550.

15. Huang DW, Sherman BT, Lempicki RA: **Systematic and integrative analysis of large gene lists using DAVID bioinformatics resources.** *Nature Protocols* 2009, **4:**44-57.

16. Huang DW, Sherman BT, Lempicki RA: **Bioinformatics enrichment tools: paths toward the comprehensive functional analysis of large gene lists.** *Nucleic Acids Research* 2008, **37:**1-13.

17. Szklarczyk D, Gable AL, Lyon D, Junge A, Wyder S, Huerta-Cepas J, Simonovic M, Doncheva NT, Morris JH, Bork P, et al: **STRING v11: protein-protein association networks with increased coverage, supporting functional discovery in genome-wide experimental datasets.** *Nucleic Acids Res* 2019, **47:**D607-d613.

18. Shannon P, Markiel A, Ozier O, Baliga NS, Wang JT, Ramage D, Amin N, Schwikowski B, Ideker T: **Cytoscape: a software environment for integrated models of biomolecular interaction networks.** *Genome Res* 2003, **13:**2498-2504.

19. Bader GD, Hogue CW: **An automated method for finding molecular complexes in large protein interaction networks.** *BMC Bioinformatics* 2003, **4:**2.

20. Chin CH, Chen SH, Wu HH, Ho CW, Ko MT, Lin CY: **cytoHubba: identifying hub objects and sub-networks from complex interactome.** *BMC Syst Biol* 2014, **8 Suppl 4:**S11.

21. Whitfield ML, Sherlock G, Saldanha AJ, Murray JI, Ball CA, Alexander KE, Matese JC, Perou CM, Hurt MM, Brown PO, Botstein D: **Identification of genes periodically expressed in the human cell cycle and their expression in tumors.** *Mol Biol Cell* 2002, **13:**1977-2000.

22. Liberzon A, Birger C, Thorvaldsdóttir H, Ghandi M, Mesirov JP, Tamayo P: **The Molecular Signatures Database (MSigDB) hallmark gene set collection.** *Cell Syst* 2015, **1:**417-425.

23. Subramanian A, Tamayo P, Mootha VK, Mukherjee S, Ebert BL, Gillette MA, Paulovich A, Pomeroy SL, Golub TR, Lander ES, Mesirov JP: **Gene set enrichment analysis: a knowledge-based approach for interpreting genome-wide expression profiles.** *Proc Natl Acad Sci U S A* 2005, **102:**15545-15550.

24. Efremova M, Vento-Tormo M, Teichmann SA, Vento-Tormo R: **CellPhoneDB: inferring cell–cell communication from combined expression of multi-subunit ligand–receptor complexes.** *Nature Protocols* 2020, **15:**1484-1506.

25. Vento-Tormo R, Efremova M, Botting RA, Turco MY, Vento-Tormo M, Meyer KB, Park J-E, Stephenson E, Polański K, Goncalves A, et al: **Single-cell reconstruction of the early maternal–fetal interface in humans.** *Nature* 2018, **563:**347-353.

26. Jin S, Guerrero-Juarez CF, Zhang L, Chang I, Ramos R, Kuan CH, Myung P, Plikus MV, Nie Q: **Inference and analysis of cell-cell communication using CellChat.** *Nat Commun* 2021, **12:**1088.

27. Chen W, Lv X, Liu C, Chen R, Liu J, Dai H, Zou GM: **Hematopoietic stem/progenitor cell differentiation towards myeloid lineage is modulated by LIGHT/LIGHT receptor signaling.** *J Cell Physiol* 2018, **233:**1095-1103.

28. Janzen V, Forkert R, Fleming HE, Saito Y, Waring MT, Dombkowski DM, Cheng T, DePinho RA, Sharpless NE, Scadden DT: **Stem-cell ageing modified by the cyclin-dependent kinase inhibitor p16INK4a.***Nature* 2006, **443:**421-426.

29. Nygren JM, Bryder D: **A novel assay to trace proliferation history in vivo reveals that enhanced divisional kinetics accompany loss of hematopoietic stem cell self-renewal.***PLoS One* 2008, **3:**e3710.

30. Kowalczyk MS, Tirosh I, Heckl D, Rao TN, Dixit A, Haas BJ, Schneider RK, Wagers AJ, Ebert BL, Regev A: **Single-cell RNA-seq reveals changes in cell cycle and differentiation programs upon aging of hematopoietic stem cells.***Genome Res* 2015, **25:**1860-1872.

31. Dumble M, Moore L, Chambers SM, Geiger H, Van Zant G, Goodell MA, Donehower LA: **The impact of altered p53 dosage on hematopoietic stem cell dynamics during aging.***Blood* 2007, **109:**1736-1742.

32. Jung H, Kim MJ, Kim DO, Kim WS, Yoon SJ, Park YJ, Yoon SR, Kim TD, Suh HW, Yun S, et al: **TXNIP maintains the hematopoietic cell pool by switching the function of p53 under oxidative stress.***Cell Metab* 2013, **18:**75-85.

33. Kanehisa M, Goto S: **KEGG: kyoto encyclopedia of genes and genomes.***Nucleic Acids Res* 2000, **28:**27-30.

34. McCabe A, Brendel C, Frei S, Klatt D, Bentler M, Snapper S, Williams DA: **Interleukin-10 Signaling in Hematopoietic Stem and Progenitor Cells Maintains Stem Cell Function and Regulates Inflammation-Induced Myeloid Cell Output.***Blood* 2018, **132:**2407-2407.

35. Wei W, Ayad NG, Wan Y, Zhang GJ, Kirschner MW, Kaelin WG, Jr.: **Degradation of the SCF component Skp2 in cell-cycle phase G1 by the anaphase-promoting complex.***Nature* 2004, **428:**194-198.

36. Imaki H, Nakayama K, Delehouzee S, Handa H, Kitagawa M, Kamura T, Nakayama KIJCr: **Cell cycle-dependent regulation of the Skp2 promoter by GA-binding protein.** 2003, **63:**4607-4613.

37. Wang HH, Lee YN, Su CH, Shu KT, Liu WT, Hsieh CL, Yeh HI, Wu YJ: **S-Phase Kinase-associated Protein-2 Rejuvenates Senescent Endothelial Progenitor Cells and Induces Angiogenesis in Vivo.***Sci Rep* 2020, **10:**6646.

38. Franceschi C, Campisi J: **Chronic inflammation (inflammaging) and its potential contribution to age-associated diseases.***J Gerontol A Biol Sci Med Sci* 2014, **69 Suppl 1:**S4-9.

39. Franceschi C, Capri M, Monti D, Giunta S, Olivieri F, Sevini F, Panourgia MP, Invidia L, Celani L, Scurti M, et al: **Inflammaging and anti-inflammaging: a systemic perspective on aging and longevity emerged from studies in humans.***Mech Ageing Dev* 2007, **128:**92-105.

40. Shavlakadze T, Morris M, Fang J, Wang SX, Zhu J, Zhou W, Tse HW, Mondragon-Gonzalez R, Roma G, Glass DJ: **Age-Related Gene Expression Signature in Rats Demonstrate Early, Late, and Linear Transcriptional Changes from Multiple Tissues.***Cell Rep* 2019, **28:**3263-3273.e3263.

41. He H, Xu P, Zhang X, Liao M, Dong Q, Cong T, Tang B, Yang X, Ye M, Chang Y, et al: **Aging-induced IL27Ra signaling impairs hematopoietic stem cells.***Blood* 2020, **136:**183-198.

42. Zhao JL, Ma C, O'Connell RM, Mehta A, DiLoreto R, Heath JR, Baltimore D: **Conversion of danger signals into cytokine signals by hematopoietic stem and progenitor cells for regulation of stress-induced hematopoiesis.***Cell Stem Cell* 2014, **14:**445-459.
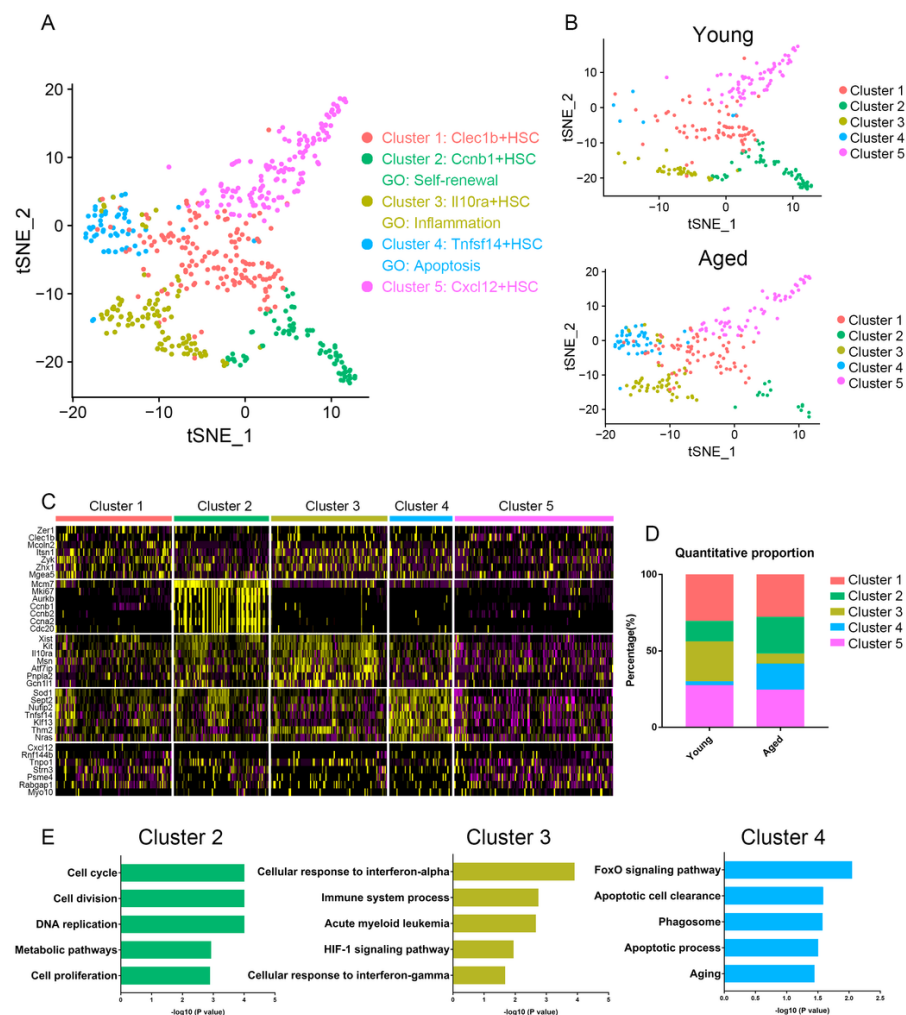
Figures

Figure 1

Cellular heterogeneity within young and aged HSCs. (A-B) T-SNE plot of HSCs analyzed using Seurat. Colors marked the 5 distinct clusters identified by unsupervised clustering and characterized with differential gene expression and gene set enrichment analyses. Each dot represents a cell. (C) Heatmap of the most significant DEGs during aging (p value < 0.01 and log fold change > 0.25 in at least one cluster) in the different clusters revealed by Seurat analysis. (D) Quantitative proportions of different clusters in young and aged HSCs. (E) Functional enrichment (biological process and KEGG pathways enrichment) of DEGs of Cluster 2, Cluster 3 and Cluster 4.

Figure 2

Identification of common differentially expressed genes (DEGs) in 3 independent single-cell transcriptome datasets (GSE100906, GSE70657, and GSE100426). (A) Heatmap of the top 100 DEGs (50 upregulated and 50 downregulated genes). (B) Common DEGs in the 3 datasets (56 upregulated and 51 downregulated genes). (C) qRT-PCR results of the relative gene expression of top 30 DEGs. Data are presented as the mean ± SEM. *p < 0.05; **p < 0.01; ***p < 0.001.
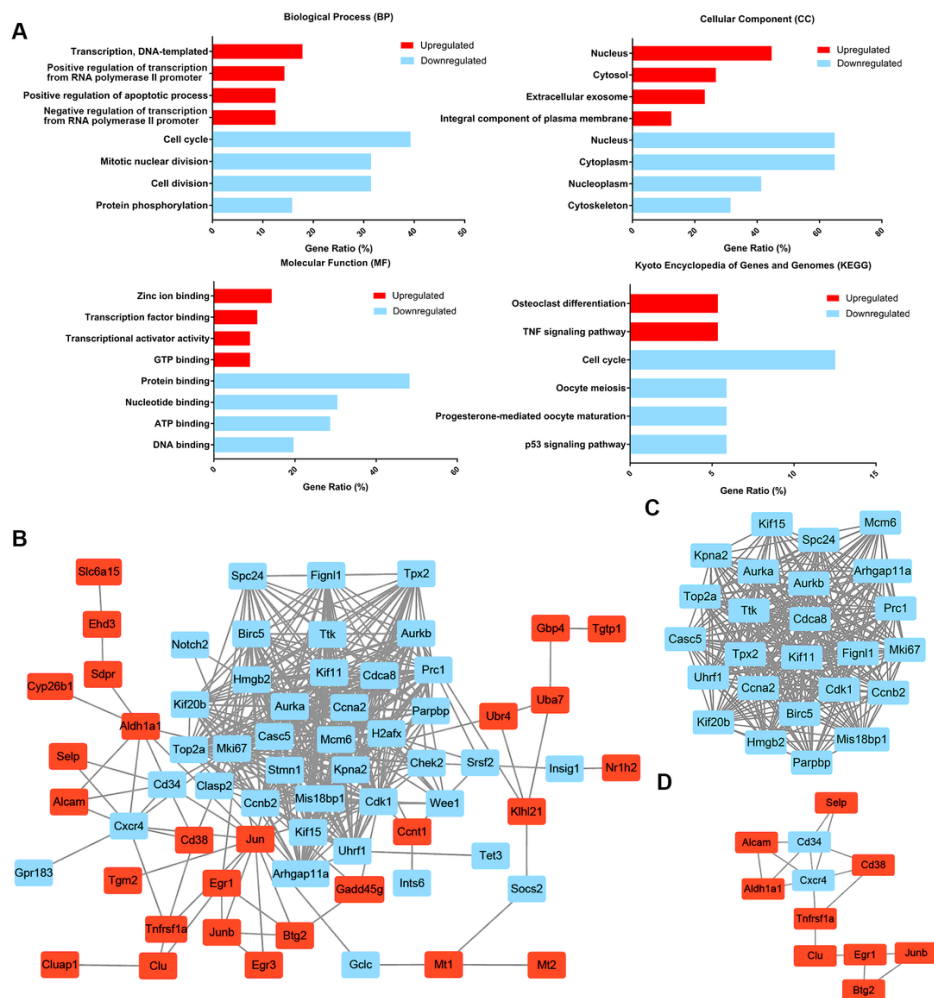
Figure 3

Functional enrichment and protein–protein interaction (PPI) network analysis of common DEGs. (A) Functional enrichment included biological process, cellular component, molecular function and Kyoto Encyclopedia of Genes and Genomes (KEGG) pathways enrichment. The gene ratio was acquired from the DAVID functional annotation tool. (B) The common DEG protein–protein interaction (PPI) network contained 67 nodes and 413 edges. (C) Two significant modules were identified based on the degree of importance. Module 1 contained 25 nodes and 286 edges and was mainly involved in the cell cycle. (D) Module 2 contained 11 nodes and 17 edges and was mainly involved in cell adhesion molecules and the hematopoietic cell lineage. Upregulated nodes are labeled in red and downregulated nodes are labeled in blue.
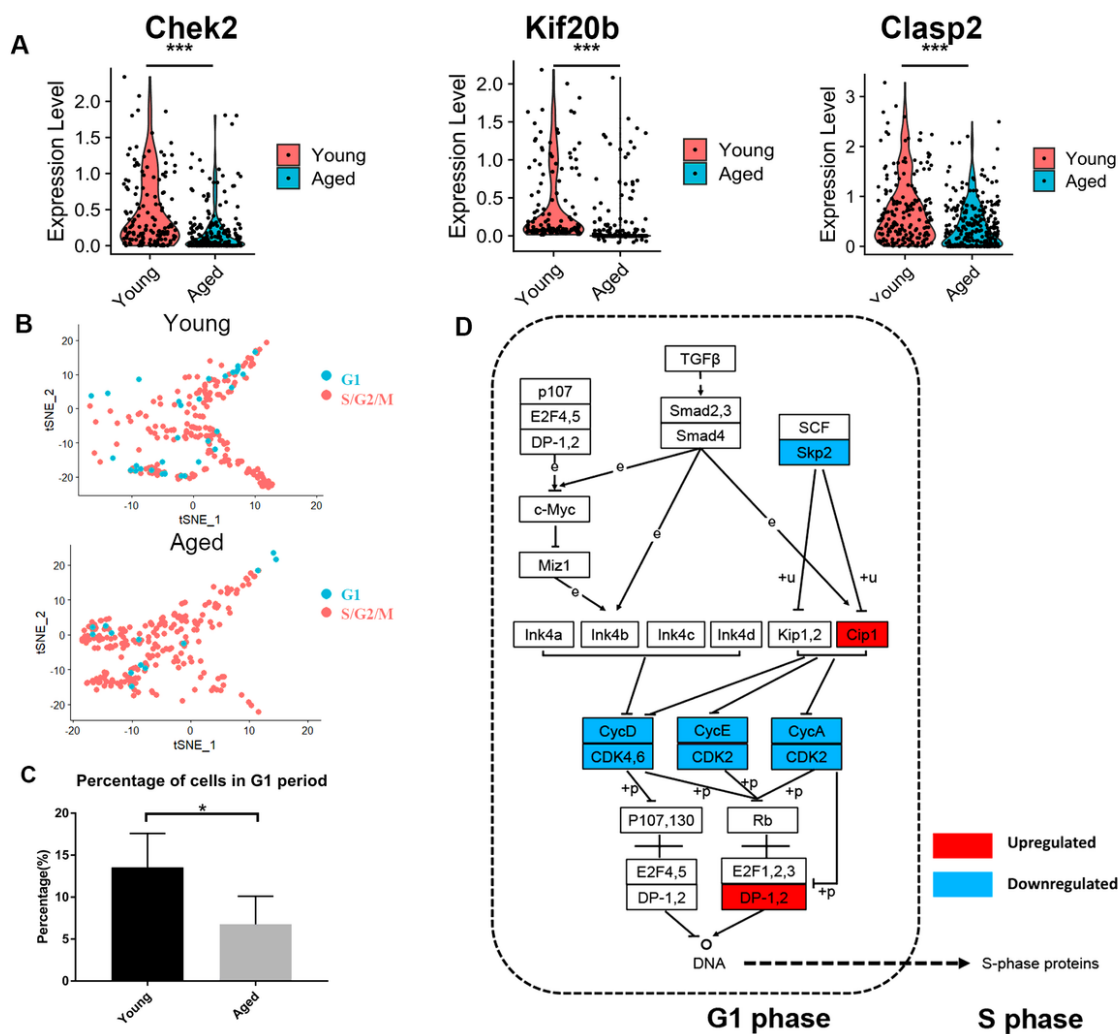
Figure 4

Cell cycle analysis of HSCs. (A) Violin plot showing the expression levels of cell cycle-associated genes (Chek2, Kif20b and Clasp2) in young and aged HSCs. (B) T-SNE plot for young and aged HSCs. (C) Histogram of cell frequency in the G1 cluster. Data are presented as the mean ± SEM. *p < 0.05. (D) Cell cycle pathway diagram showing alterations in signaling pathway activity. Downregulation of the Skp2-induced signaling pathway (Skp2→Cip1→CycA/CDK2→DP-1) promoted the transition from G1 phase to S phase. Upregulated genes are labeled in red and downregulated genes are labeled in blue.
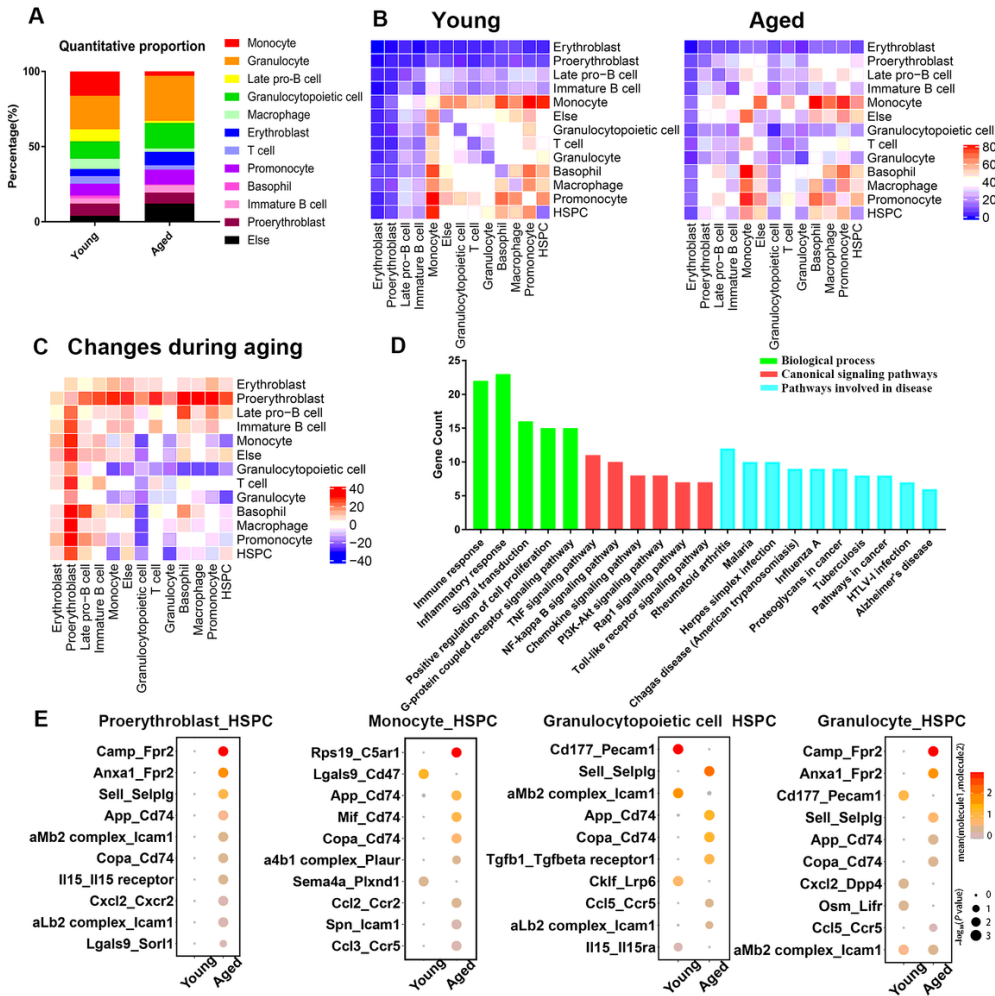
Figure 5

Cellular composition and interactions between HSCs and other cell types in the bone marrow niche. (A) Quantitative proportions of different cell types in the bone marrow niche. (B) Heatmap showing the number of interactions between different cell types in young and aged bone marrow separately. (C) Heatmap showing the differences in the number of interactions (interaction number of aged cells minus the interaction number of young cells). (D) Functional enrichment results for differentially expressed ligand–receptor pairs. (E) Dot plots showing the ligand–receptor pairs between the ligand of proerythroblasts/monocytes/granulocytopoietic cells/granulocytes and the receptor of HSPCs in young and aged mice. The color of the dots represents the mean expression of each ligand and receptor, and the size of the dots represents -log10(P value).
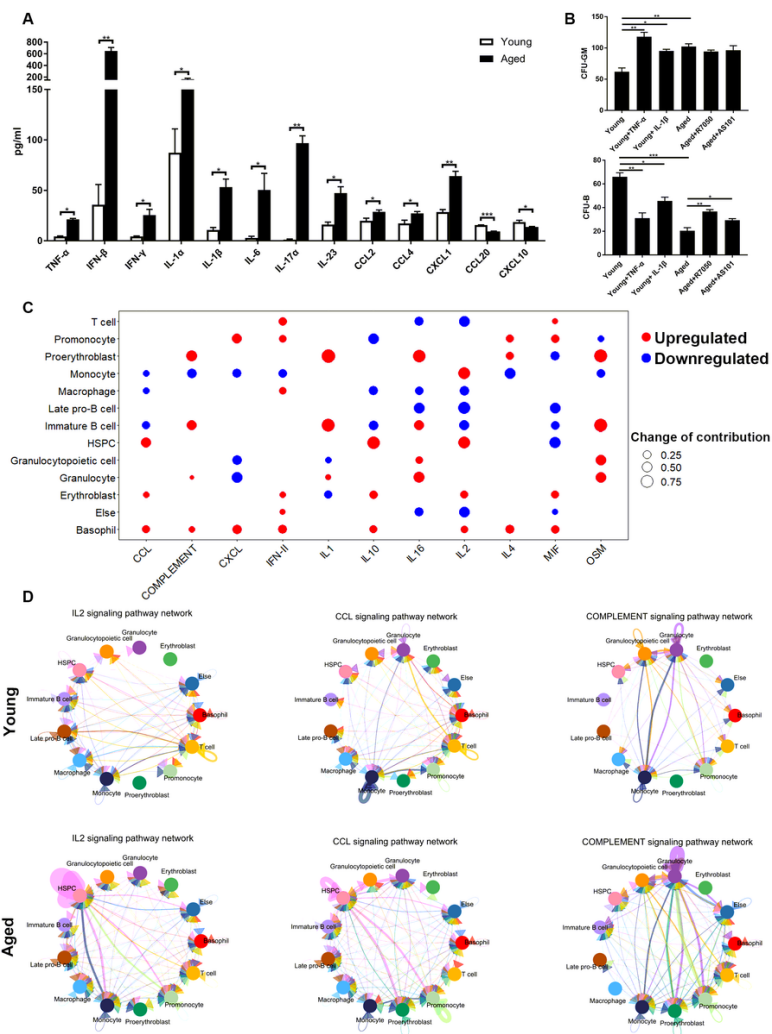
Figure 6

Inflammation-related cytokines and chemokines in the bone marrow niche. (A) Quantitation of inflammation-related cytokines and chemokines in young and aged bone marrow niches via a Cytoplex Assay. Data are presented as the mean ± SEM.*p < 0.1; **p < 0.01; ***p < 0.001. (B) Ganulocyte/macrophage (GM) and B cell colony formation was measured for young or aged HSPCs incubated for 10 days in methylcellulose in the presence of either DMSO vehicle or IL-1β (25 ng/ml), TNF-α (1 µg/ml), AS101 (2µg/ml, IL-1β inhibitor) and R7050 (2µg/ml, TNF-α receptor antagonist). Graph shows mean±SEM. (C) Dot plots showing the differences in the contribution to different inflammation-related signaling pathways. Upregulated cytokines and chemokines are labeled in red and downregulated cytokines and chemokines are labeled in blue. The size of the dots represents the change in contribution. (D) Circle plot of the cell-cell communication network showing that the inflammatory pathway network (IL2, CCL and complement signaling pathways) became more complex and interconnected in the aged bone marrow niche.

Supplementary Files

This is a list of supplementary files associated with this preprint. Click to download.

- SupplementaryFigure1.tif
- SupplementaryTable1.docx
- SupplementaryTable2.docx
- SupplementaryTable3.docx